

Model-independent Reconstruction of UV Luminosity Function and Reionization Epoch

Debabrata Adak,^{a,b,c,d} Dhiraj Kumar Hazra,^{c,d,e} Sourav Mitra,^f
Aditi Krishak^{c,g}

^aInstituto de Astrofísica de Canarias, E-38200 La Laguna, Tenerife, Spain

^bDepartamento de Astrofísica, Universidad de La Laguna, E-38206 La Laguna, Tenerife, Spain

^cThe Institute of Mathematical Sciences, CIT Campus, Chennai 600113, India

^dHomi Bhabha National Institute, Training School Complex, Anushakti Nagar, Mumbai 400085, India

^eINAF/OAS Bologna, Osservatorio di Astrofisica e Scienza dello Spazio di Bologna, via Gobetti 101, I-40129 Bologna, Italy

^fDepartment of Physics, Surendranath College, 24/2 M. G. Road, Kolkata 700009, India

^gDepartment of Physics and Astronomy, University of Southern California, University Park, Los Angeles, CA 90089, USA

E-mail: adak@iac.es, dhiraj@imsc.res.in, hisourav@gmail.com, krishak@usc.edu

Abstract. We conduct a first comprehensive study of the Luminosity Function (LF) using a non-parametric approach. We use Gaussian Process to fit available luminosity data between redshifts $z \sim 2 - 8$. Our free-form LF in the non-parametric approach rules out the conventional Schechter function model to describe the abundance-magnitude relation at redshifts $z = 3$ and 4. Hints of deviation from the Schechter function are also noticed at redshifts 2, 7 and 8 at lower statistical significance. Significant deviation starts for brighter ionizing sources at $M_{UV} \lesssim -21$. The UV luminosity density data at different redshifts are then derived by integrating the LFs obtained from both methods with a truncation magnitude of -17 . In our analysis, we also include the first 90 arcmin² JWST/NIRCam data at $z \sim 9 - 12$. Since at larger magnitudes, we do not find major deviations from the Schechter function, the integrated luminosity density differs marginally between the two methods. Finally, we obtain the history of reionization from a joint analysis of UV luminosity density data along with the ionization fraction data and Planck observation of Cosmic Microwave Background. The history of reionization is not affected by the deviation of LFs from Schechter function at lower magnitudes. We derive reionization optical depth to be $\tau_{re} = 0.0494_{-0.0006}^{+0.0007}$ and the duration between 10% and 90% completion of ionization process is found to be $\Delta z \sim 1.627_{-0.071}^{+0.059}$.

Keywords: Galaxy Luminosity function - Gaussian process (GP) - Reionization history

Contents

| | | |
|----------|---|-----------|
| 1 | Introduction | 1 |
| 2 | Methodology | 3 |
| 2.1 | Cosmic Reionization | 3 |
| 2.2 | Gaussian Process Regression | 4 |
| 3 | Data sets | 5 |
| 4 | Results | 5 |
| 4.1 | Relation between magnitude and Galaxy UV LF | 5 |
| 4.2 | Evolution of UV Luminosity Density | 7 |
| 4.3 | Constraints on Reionization | 8 |
| 5 | Summary | 12 |
| 6 | Acknowledgement | 13 |
| A | Modification to the mean functions due to changes in the hyperparameters | 13 |

1 Introduction

The process of cosmic reionization is an outstanding problem in extragalactic astronomy. During the redshifts $z \sim 6 - 20$ almost all of the hydrogen in the universe became ionized [1–5]. A similar process was followed for helium at a later time and helium reionization was completed at around $z \sim 2.5 - 3.5$ [6]. For this process, the high-redshift ($z \gtrsim 6$) star-forming galaxies are often considered to be the dominant contributors of ionizing photons since the abundance of quasars dramatically declines at $z \sim 6$ [7–9]. A variety of theoretical and observational studies have shown that the contribution of Active Galactic Nuclei has a very minimal ($\lesssim 1\%$) contribution to the total ionisation budget at $z \geq 6$ [10, 11]. Most of the studies suggest that star-forming galaxies inside the low mass halo ($M_h \lesssim 10^{9.5} M_\odot$) are sufficient enough to complete the reionization process [12, 13]. Therefore, their time-dependent abundance, and the redshift evolution of UV luminosity density (ρ_{UV}) derived from rest-frame UV luminosity function (LF) of galaxies are of significant interest for understanding reionization history (see, [14]).

Significant advancement has been made in determining the behaviour of LFs at redshifts $z \sim 4 - 10$ using Hubble Frontier Fields (HFF, [15]) survey data up to magnitude $\simeq -15$ [16–18]. More recently, the same has been studied in [19, 20] and [21] with galaxy candidates down to magnitude $\simeq -22$. However, along with studying the faint end of the UV LF, it is also important to investigate the bright-end shape of LF. While the conventional Schechter function [22] seems to be a good description of the LFs for ionizing candidates at the fainter end of the magnitude, an exponential decline has been reported in their number densities at the bright-end [23]. It is thought to be caused by heating from an active galactic nucleus (AGN, [24]), inefficient cooling of gas inside high-mass dark matter halos at low redshifts [25] etc. The studies in [26, 27] and [28] reported an excess of number density compared to that described by the Schechter best fit at $z \sim 4 - 7$.

With the improvement of signal-to-noise ratio in astrophysical observations, search for beyond standard model has usually taken two approaches, namely, model building and model independent reconstructions. In this paper, for the first time, we search for the deviations beyond Schechter function using model independent approach. Model building approaches follow either phenomenological or theoretical constructions. Recent works of [26] and [29] found that both double power-law (DPL, [30]) and lensed Schechter function [31] are better fit to the UV luminosity data. Their studies include brightest galaxy candidates observed in the early data from James Webb Space Telescope (JWST, [32]) and Great Optically Luminous Dropout Research data of Subaru HSC (GOLDRUSH) (corrected for AGN contribution) respectively. Publications [33] and [34] independently established that LFs are more consistent with DPL at $z \sim 9 - 10$. DPL model is a simple modification of Schechter function with introduction of another power law (see Eq.1 of [30]) instead of exponential decrease of Schechter form after a certain magnitude. The lensed Schechter function is a convolution of magnification effect on the observed shape of the galaxy UV luminosity function determined by intrinsic Schechter function. This magnification bias is determined by strong-lensing optical depth that is fraction of strong-lensed random lines of sight. In current literature [29] the amount of modification is based on upper limit of optical depth by foreground sources estimated in [35, 36] along with pre-determined Schechter parameters. These parameterization allows us to find any excess or drop in abundance at a certain end of magnitude. However, these approaches restrict the flexibility to determine the actual trend of luminosity-magnitude relation throughout the scale of magnitude. Model independent approach here helps in highlighting the significance of the outliers and the hints for model building. The Gaussian process (GP) is a Bayesian model independent reconstruction that provides the possible departure from the Schechter function throughout the scale of the magnitude. The GP hyperparameters directly highlight the significance with which the data disfavors the Schechter function. It also finds the short range or long range nature of the deviation of LF from parametric models.

In this paper, we address the constraints on reionization history in a two-step process. First, we reconstruct the profile of the LFs using GP, a nonparametric Bayesian method at redshifts $z \sim 2 - 8$, and Schechter function model at redshifts $z \sim 2 - 12$ using the HFF data, early JWST data and HSC data. We compare these model-independent LFs with the best fit Schechter function model. We derive the UV luminosity densities by integrating LFs, and investigate the redshift evolution of UV luminosity densities derived from both profiles. Finally, we use these luminosity densities to constrain the history of reionization along with jointly fitting two other observational data: the CMB power spectrum data of temperature and polarization anisotropy from Planck observation [4] and neutral hydrogen fraction data from galaxy, quasar and gamma-ray burst observations.

The paper is organised as follows. In [section 2](#) we briefly discuss the reionization process, different functions used and details of Gaussian process regression. In [section 3](#) we describe the ancillary data sets used in this work. In [section 4](#) we present our results for the UV luminosity functions obtained using two different methods, their comparison, derived UV luminosity densities and the corresponding constraints on reionization history. Finally in [section 5](#) we summarise the work.

2 Methodology

2.1 Cosmic Reionization

The process of reionization of the intergalactic medium (IGM) is a balance between ionization of hydrogen and helium atoms by cosmic photons and recombination of free electrons and protons to form neutral hydrogen and helium. Analytical and numerical modelling of this process traces a long history [13, 37, 38] (see the references therein). The process is studied by the redshift evolution of volume filling factor Q_{HII} which is governed by the ionization histories of both hydrogen and helium. The time evolution of Q_{HII} is obtained by solving the ordinary differential equation (e.g. [39])

$$\dot{Q}_{\text{HII}} = \frac{\dot{n}_{\text{ion}}}{\langle n_H \rangle} - \frac{Q_{\text{HII}}}{t_{\text{rec}}}, \quad (2.1)$$

where $\langle n_H \rangle = \frac{X_p \Omega_b \rho_c}{m_H}$ is the mean comoving number density of hydrogen and depends on the primordial mass-fraction of hydrogen X_p , critical density ρ_c , baryon density Ω_b and m_H is the mass of atomic hydrogen. t_{rec} denotes the average recombination time in the IGM,

$$t_{\text{rec}} = \frac{1}{C_{\text{HII}} \alpha_B(T) \left(1 + \frac{Y_p}{4X_p}\right) \langle n_H \rangle (1+z)^3}, \quad (2.2)$$

where $\alpha_B(T)$ is the recombination coefficient for hydrogen (we assume the IGM temperature T to be 20,000 K) and $Y_p = 1 - X_p$ is the primordial helium abundance. The clumping factor C_{HII} accounts for the inhomogeneity of the IGM, and is not very well constrained from observations. Recent simulations suggest a possible range of C_{HII} value from 1 to 6 [40–43]. In this work we use the fixed value of $C_{\text{HII}} = 3$ [44] for simplicity. The comoving production rate of available ionizing photons in the IGM at some redshift is

$$\begin{aligned} \dot{n}_{\text{ion}} &= \int_{-\infty}^{M_{\text{trunc}}} f_{\text{esc}}(M) \xi_{\text{ion}}(M) \Phi(M) L(M) dM \\ &= \langle f_{\text{esc}} \xi_{\text{ion}} \rangle \rho_{\text{UV}}. \end{aligned} \quad (2.3)$$

This depends on the intrinsic production rate of Lyman continuum (LyC) photons supplied by stellar populations of galaxies, which is parameterized by a numerical factor ξ_{ion} to count the ionizing photons per unit UV luminosity, the escape fraction f_{esc} and total luminosity density ρ_{UV} from star-forming galaxies with a truncation absolute magnitude M_{trunc} . f_{esc} is a crucial parameter and is not well-constrained from direct observations of LyC photons [45], which is mainly limited to $z \sim 2 - 4.5$ due to a dramatic increase in the opacity of IGM at high redshifts making direct observation of LyC photons difficult [46]. Moreover, the trend of f_{esc} with halo mass is not well understood from theoretical modelling [47–49]. All pre-JWST literatures suggest that a low ionisation efficiency of around $\log_{10} \xi_{\text{ion}} = 25.2 \text{ Hz erg}^{-1}$ and hence f_{esc} of 0.2 [39] that are sufficient to give reionization history consistent with CMB data. However new JWST data suggests a higher ξ_{ion} [50] that increases at redshifts higher than $z \sim 9$ [51, 52]. It is apparent that ξ_{ion} and f_{esc} are completely degenerate parameters. A recent data-driven model-independent study [53] found that a constant value of f_{esc} for $z \geq 6$ is permitted. Therefore, we take f_{esc} as a constant factor and, instead of considering ξ_{ion} and f_{esc} to be independent parameters, we consider the magnitude-averaged value of $\langle f_{\text{esc}} \xi_{\text{ion}} \rangle$ as a single parameter in this work.

Luminosity density ρ_{UV} is obtained from the luminosity function $\phi(M_{\text{UV}})$ via integration,

$$\rho_{\text{UV}} = \int_{-\infty}^{M_{\text{trunc}}} \Phi(M)L(M)dM, \quad (2.4)$$

where $L(M)$ is the luminosity. One can set the truncation magnitude at $M_{\text{trunc}} = -10$ corresponding to the predicted range of minimum halo-mass that can host star-forming galaxies [54]. However, due to insufficient data at some redshifts at larger magnitudes ($M_{\text{UV}} > -17$), our free-form LFs obtained using GP will be biased to the mean function beyond the range of training data. Therefore, we restrict ourselves to $M_{\text{trunc}} = -17$. Accurate estimation of ρ_{UV} from UV galaxies requires a careful analysis of the LF profile that can well-describe the number densities of star-forming galaxy samples down to observed limits. The best model of LF in literature is often assumed to be the Schechter function [22],

$$\Phi(M) = 0.4 \ln 10 \phi^* [10^{0.4(M^*-M)}]^{1+\alpha} \exp[-10^{0.4(M^*-M)}] \quad (2.5)$$

parameterized by ϕ^* ($\text{Mpc}^{-3}\text{mag}^{-1}$), M^* and α . We find the posterior distributions of Schechter function parameters in redshifts $z \sim 2 - 12$ using the UV luminosity data sets described in section 3. We also fit same data sets using the non-parametric method discussed in subsection 2.2. We then obtain ρ_{UV} corresponding to each of these best-fit LFs using Equation 2.5.

In order to constrain the reionization process, we need to adopt a parametric form [19, 20, 55] or a free-form [56–59] of ρ_{UV} evolution to constrain \dot{n}_{ion} . The model-independent reconstruction of reionization process in [58] rules out the single power-law [55] form which that is unable to replicate the decline at $z \sim 8$. This results in an incorrect value of the Thomson scattering optical depth. Therefore, in our analysis we use the logarithmic double power law [19, 20] to describe ρ_{UV} ,

$$\rho_{\text{UV}} = \frac{2\rho_{\text{UV},z=z_{\text{tilt}}}}{10^{a(z-z_{\text{tilt}})} + 10^{b(z-z_{\text{tilt}})}}, \quad (2.6)$$

where $\rho_{\text{UV},z=z_{\text{tilt}}}$ is the normalization factor at $z_{\text{tilt}} \sim 8$, and a and b are the slopes.

Once the evolution of Q_{HII} from Eq. 2.1 is determined, we compute the reionization optical depth at redshift z using

$$\tau_{\text{re}} = \int_0^z \frac{c(1+z')^2}{H(z')} Q_{\text{HII}}(z') \langle n_H \rangle \sigma_T (1 + \eta \frac{Y_p}{4X_p}) dz', \quad (2.7)$$

where c is the speed of light, $H(z)$ is the Hubble parameter, and σ_T is the Thomson scattering cross section. Here we assume that helium is singly ionized ($\eta = 1$) at $z > 4$ and doubly ionized ($\eta = 2$) at $z \leq 4$ [38].

2.2 Gaussian Process Regression

Gaussian process regression is a non-parametric Bayesian regression method. This method has been extensively used in cosmological data analysis [60–62]. A Gaussian process is a collection of random variables such that any finite subset of these random variables has a multivariate Gaussian distribution [63]. A GP is described by its mean and covariance functions, defined as $\mu(X) = \mathbb{E}[f(X)]$, and $k(X, X') = \mathbb{E}[(f(X) - \mu(X))(f(X') - \mu(X'))]$, respectively, for a real process $f(X)$. In particular, here $f(X)$ defines the luminosity-magnitude

relation guided by data for a given mean function. The covariance function gives the covariance between two random variables and characterizes the covariance matrix having elements $C_{i,j} = k(x_i, x_j)$. Given a finite set of training points $\mathbf{X} = \{x_i\}$, a function $f(\mathbf{X})$ evaluated at each x_i is a Gaussian random variable and the vector $\mathbf{f}(\mathbf{X}) = \{f_i\}$ has a multivariate Gaussian distribution given as $\mathbf{f}(\mathbf{X}) \sim \mathcal{N}(\boldsymbol{\mu}(\mathbf{X}), C(\mathbf{X}, \mathbf{X}))$. The choice of the covariance functions is important. We choose the Radial Basis Function (RBF) kernel as the covariance function for our analysis, defined as $K(x_i, x_j) = \sigma_\ell \exp\left(-\frac{(x_i - x_j)^2}{2\ell^2}\right)$, where σ_ℓ and ℓ are the kernel hyperparameters. The σ_ℓ is the amplitude parameter that can be thought as an offset that decides the tilt of reconstructed function $f(\mathbf{X})$ from given mean function and ℓ describes the characteristic length of correlation. The role of two hyperparameters are discussed in detail in Appendix A. Data points act as training points to optimize the hyperparameters and provide posterior prediction along with uncertainty on the predictions for the given test points.

Although GP is a formalism to be used here to study actual trends of data to define the luminosity-magnitude relation, there are practical technicalities regarding the choice of mean function that require special care. In principle, one can choose a zero mean function or any random function to start with. In this study, however, we are particularly interested in checking the validity of the Schechter function to be a correct description of the luminosity-magnitude relation. To test that, we allow the three Schechter function parameters to vary along with the GP hyperparameters, ℓ and σ_ℓ . In this way, the hyperparameter posteriors, marginalized over the Schechter function parameters can indicate, in a conservative way, whether the Schechter function is a correct model to address the observational data.

3 Data sets

We use rest frame UV luminosity function data for redshifts $z \sim 2, 3, 4, 5, 6, 7$ derived in [64] using HUDF, HFF, and CANDELS fields and HFF data compiled by [20]. For $z \sim 4-7$ we add data from Hyper Suprime-Cam (HSC) Subaru Strategic Program (SSP) survey [65]. These data sets are corrected for active galactic nucleus (AGN) contribution and mostly at brighter end of luminosity. For redshifts 8, 9 and 10 we use luminosity function data from [64], [34], [66] and [67]. We also use the data redshift 9 and 12 from JWST [68].

We use neutral hydrogen fraction data to constrain reionization from observations of Ly α -emitting galaxies [48, 69–71], high-redshift quasar spectra [43, 72, 73], gamma ray bursts [74, 75], dark fraction in the spectra of bright quasars [2] and ionized near-zones around high-redshift quasars [76, 77].

From Planck CMB, we use Planck binned Plik TTTEEE likelihood with low multipole temperature and polarization likelihoods and the lensing likelihood as discussed in Planck baseline [4].

4 Results

4.1 Relation between magnitude and Galaxy UV LF

To characterise the galaxy UV LF, we use both Schechter function (Equation 2.5) and GP to fit the luminosity data. We use data for the largest possible range of magnitude, $-25 < M_{UV} < -14$ wherever available. We use CosmoMc [78] as a generic sampler to explore the parameter space.

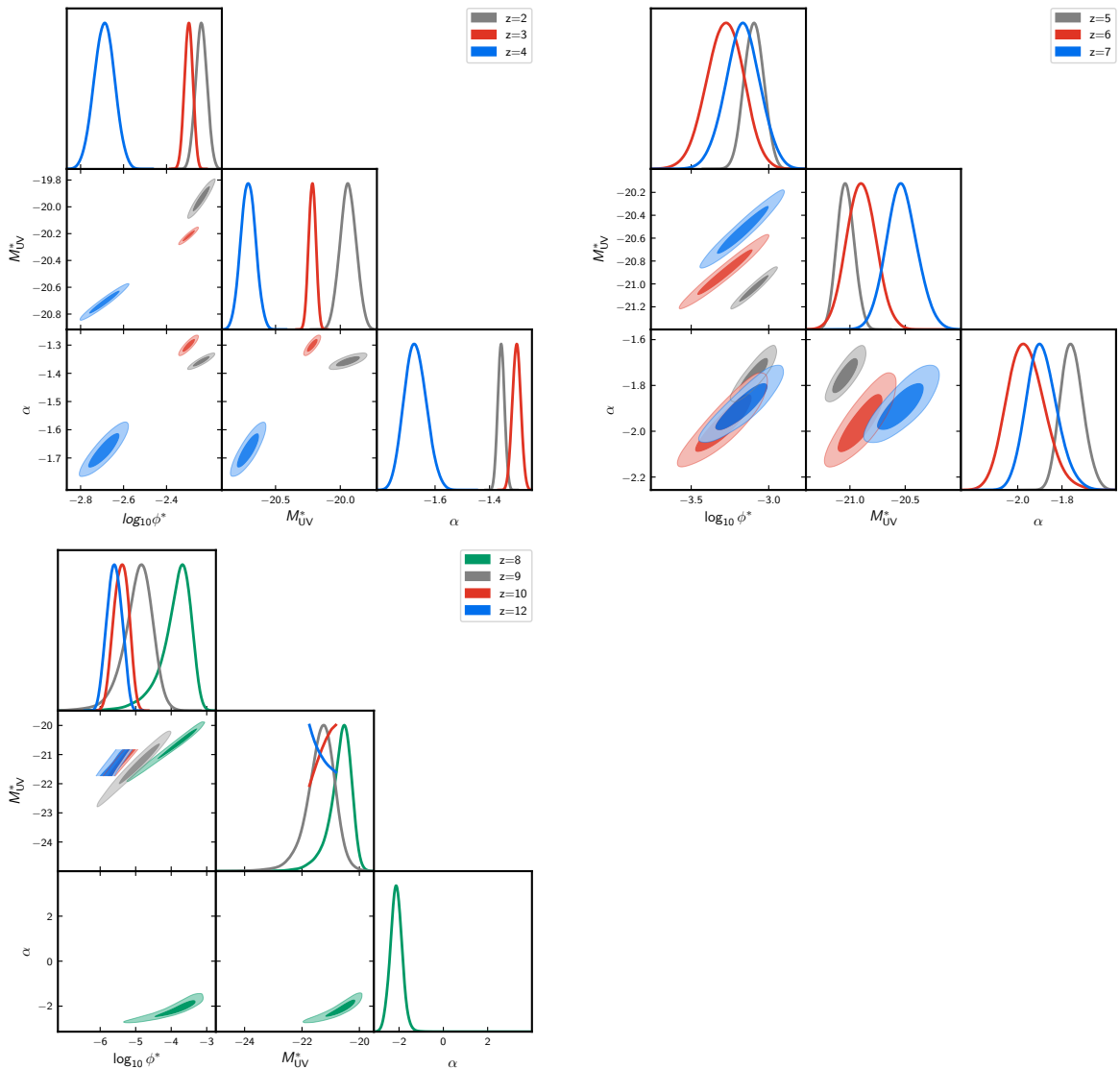


Figure 1. Constraints on the Schechter function parameters using galaxy luminosity data at redshifts $z \sim 2 - 12$.

For fitting the Schechter function we keep all three parameters M^* , ϕ^* and α free. However, we notice that for $z > 8$ the data is not able to constrain all the parameters. Therefore, at $z \geq 9$, we keep the slope α fixed at -2.35 following [29] and determine the other two Schechter parameters at $z \sim 9-12$. We find the estimated parameters are consistent with previous results of [20, 34, 64]. For $z \sim 10$ and 12, we fix the prior on M_{UV}^* as the 68% range obtained in $z \sim 9$ analysis. In Figure 1 we present posterior distributions of the Schechter function parameters. We fit the free-form of LF using GP with the same data sets keeping GP hyperparameters (ℓ and σ_ℓ) free along with three Schechter parameters. We avoid GP fitting at $z \sim 9 - 12$ due to the unavailability of low magnitude high signal-to-noise data where deviation is expected and at these redshifts, even all Schechter parameters cannot be optimised. The analysis of ten redshifts is divided into three plots. Random samples of luminosity function from the chains for Schechter function are plotted in blue lines

in [Figure 2](#) and [3](#). Modified functions from the Gaussian process are plotted in orange lines in the same figures. Deviations from Schechter function below magnitude $M_{UV} = -21$ can be noticed. A similar deviation is also reported in [\[26\]](#). It is important to note that most of the previous studies are based on HFF and HUDF data [\[20, 21, 64, 79\]](#) and others ground-based observations [\[34\]](#) that are limited by the magnitude larger than -23 . According to those studies, Schechter function is the best description of the magnitude-luminosity relation. In our study, we combine those previous data sets with ancillary luminosity data sets of brighter galaxies ($M_{UV} \lesssim -23$) from HSC data [\[29\]](#). Above this magnitude, the AGN contamination to the galaxy luminosity is negligible [\[80–84\]](#) and therefore the previous results are consistent with our results up to certain magnitudes. The added HSC data of brighter galaxies are corrected for contribution from AGNs [\[29\]](#). We find maximum excess in the bright end shape of galaxy UV LF instead of expected exponential drop of Schechter function at all redshifts where low magnitude ($M_{UV} \lesssim -21$) data are available. In certain redshifts, due to high signal-to-noise ratio, the deviation is detected at high statistical significance while for other redshifts we obtain a similar deviation with lower significance. Importantly, at $z = 3, 4$ the hyperparameters posteriors plotted in the upper left panel of [Figure 4](#) indicate that the Schechter function (used as a mean function in this analysis) is ruled out by the data at high significance. Data from $z = 2$ and 7 also prefer modification over Schechter function at around $\sim 95\%$ confidence level (C.L). In order to understand the source for this deviation, we reanalyse $z = 4$ data with two different data cuts (with $M_{UV} > -23$ and $M_{UV} > -21$). The results are presented in the lower right panel of [Figure 4](#). When the brightest part of the observation $-24 < M_{UV} < -23$ is not used, we notice a decrease in the significance in the GP hyperparameters ruling out Schechter function at 3σ . When we use more conservative cuts by masking data between $-24 < M_{UV} < -21$, we find that further drop in significance. These tests reveal that the modifications to Schechter function are needed by the luminosity observations at the lowest magnitude (the brightest) objects.

4.2 Evolution of UV Luminosity Density

We compute the UV luminosity density ρ_{UV} following [Equation 2.4](#) integrating down to $M_{UV} = -17$. The samples of LFs from Schechter and GP analyses are used to estimate the posterior distribution of the derived parameter ρ_{UV} . The mean and the 68% bounds are provided in [Table 1](#). The changes in luminosity density compared to the Schechter function model are not noticeable in the GP results. Though Schechter function is ruled out by the data at certain redshifts, the major required modifications are noticed at the brightest end of the function and the brightest end does not contribute significantly to the integral of the UV luminosity density as the function drops logarithmically with the increase in brightness. In [Figure 5](#), we plot the redshift evolution of the luminosity density obtained from the GP (and Schechter fit) and a logarithmic double power law fit to the data (for $z \geq 6$). We demonstrate only 1σ and 2σ spread for logarithmic double power-law fit to luminosity density obtained from the Schechter fit. We notice outliers in the data *w.r.t.* the model around redshifts 9 and 10. Recent JWST data suggests an enhanced population of star-forming Galaxies above redshifts $z \sim 9$ [\[85, 86\]](#). Compared to [\[58\]](#) new data may seem to hint towards a modification to the luminosity density evolution model. However, note that the data from JWST can not constrain all of the Schechter function parameters due to low signal-to-noise ratio detection, in particular, the slope remains unconstrained (see, [Figure 1](#)). This may bias the estimation of the luminosity density and therefore, with this data we avoid

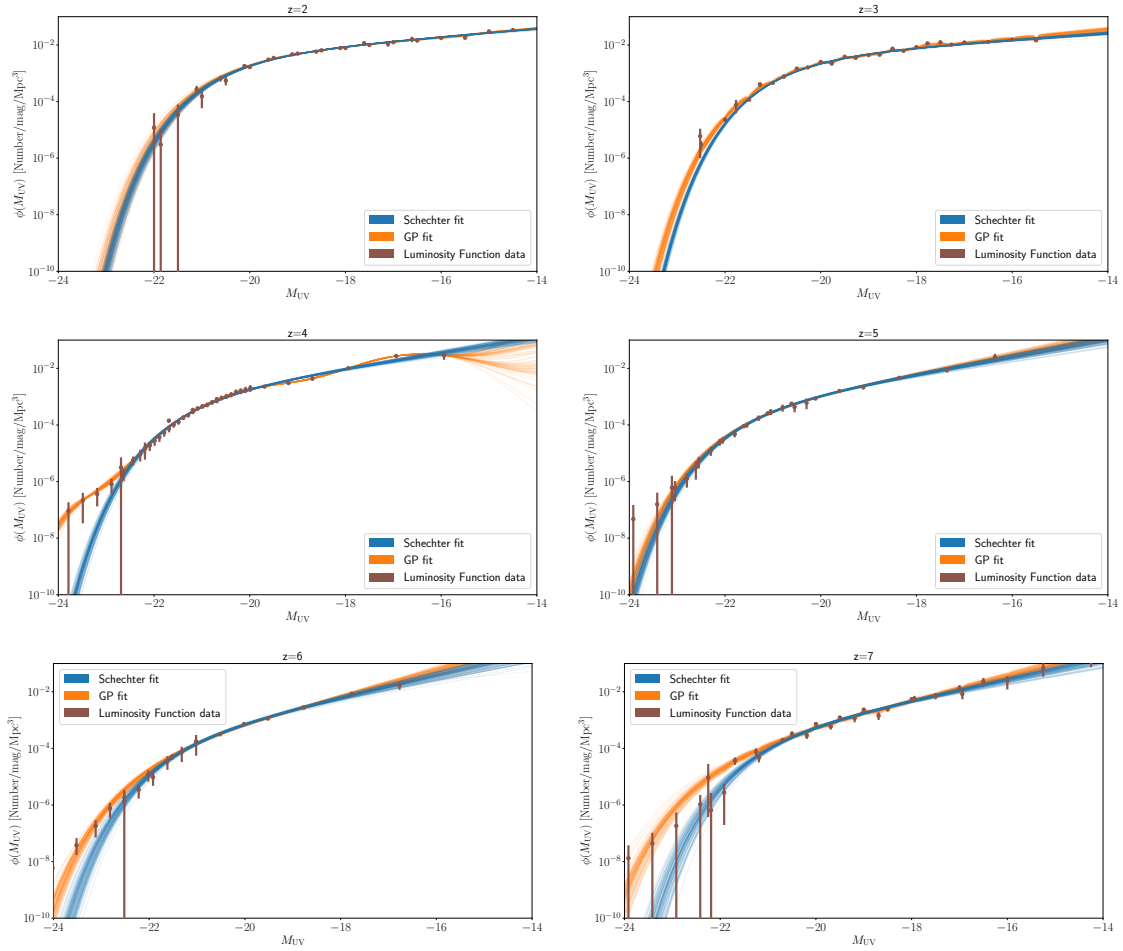


Figure 2. Comparison of luminosity functions from GP and Schechter function model derived from posterior samples of corresponding parameters at redshifts $z \sim 2 - 7$.

the exploration for the possible deviation from the double power law model. We expect to revisit this issue in the future when new data from JWST are made available.

4.3 Constraints on Reionization

We obtain the constraint on redshift evolution of IGM neutral hydrogen fraction from joint fitting of Planck data, Q_{HII} data, and UV luminosity density data derived in [subsection 4.2](#). We treat the four parameters in logarithmic double power-law form of ρ_{UV} and $\log_{10}\langle f_{\text{esc}}\xi_{\text{ion}}\rangle$ as free parameters. For C_{HII} we use a fixed value of 3.

In [Figure 6](#) we compare the Q_{HII} evolution across redshift $z \sim 4-15$ solving [Equation 2.1](#) using ρ_{UV} data sets obtained from both parametric and non-parametric methods. The blue dashed line and magenta solid line are the best fit Q_{HII} obtained with ρ_{UV} from GP and Schechter fits respectively. The grey and cyan lines indicate random samples of Q_{HII} obtained from these fits respectively. We also overplot the Q_{HII} data set used in our analysis. Both the ρ_{UV} data sets provide similar constraints on reionization history. This is not surprising as we discussed that the obtained luminosity density follows similar redshift evolution owing to the similar nature of luminosity functions at the faint source end. This result suggests that

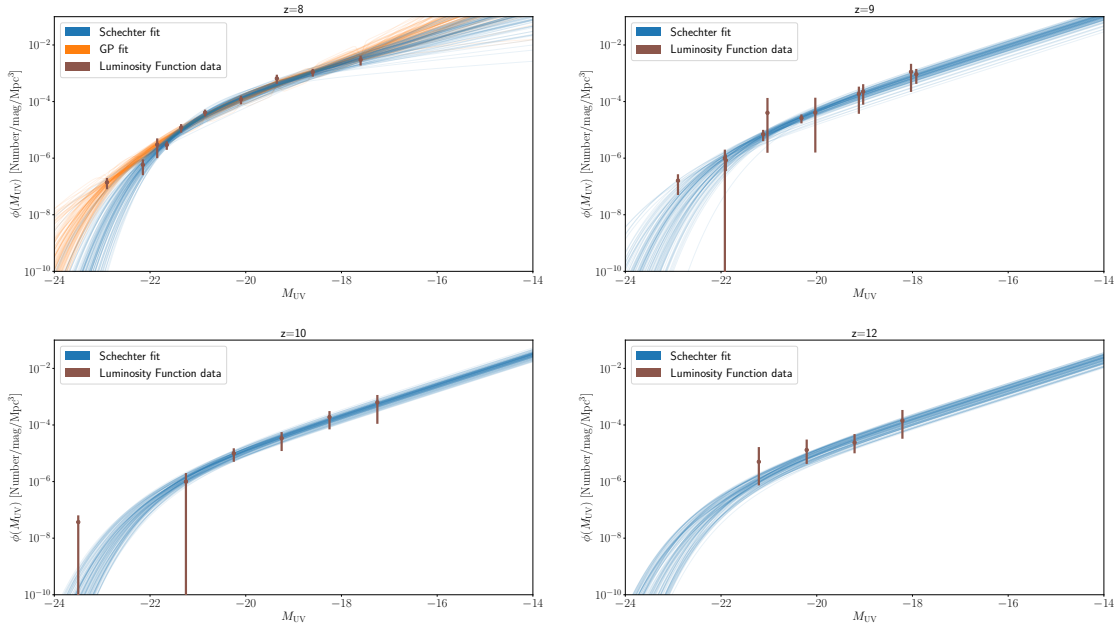


Figure 3. Same as Figure 2 for $z \sim 8, 9, 10$ and 12 .

| Model | Schechter fit | | | | Gaussian process |
|-------|-------------------------|--------------------------|----------------------------|----------------------------|----------------------------|
| | $\log_{10} \phi^*$ | M_{UV}^* | α | $\log_{10} \rho_{UV}$ | $\log_{10} \rho_{UV}$ |
| 2 | -2.238 ± 0.026 | -19.940 ± 0.061 | -1.357 ± 0.012 | 26.426 ± 0.010 | 26.436 ± 0.012 |
| 3 | -2.297 ± 0.019 | -20.216 ± 0.027 | -1.301 ± 0.015 | 26.4741 ± 0.0063 | $26.489^{+0.014}_{-0.012}$ |
| 4 | -2.689 ± 0.047 | -20.711 ± 0.057 | -1.673 ± 0.040 | 26.470 ± 0.014 | 26.470 ± 0.013 |
| 5 | -3.095 ± 0.062 | -21.039 ± 0.077 | $-1.755^{+0.047}_{-0.055}$ | 26.264 ± 0.019 | 26.275 ± 0.016 |
| 6 | -3.28 ± 0.12 | -20.90 ± 0.13 | $-1.962^{+0.076}_{-0.091}$ | $26.165^{+0.033}_{-0.028}$ | $26.188^{+0.022}_{-0.026}$ |
| 7 | -3.17 ± 0.11 | -20.53 ± 0.14 | $-1.890^{+0.062}_{-0.074}$ | 26.039 ± 0.022 | $26.071^{+0.034}_{-0.023}$ |
| 8 | $-3.88^{+0.51}_{-0.23}$ | $-20.68^{+0.46}_{-0.24}$ | -2.13 ± 0.27 | $25.616^{+0.099}_{-0.066}$ | 25.705 ± 0.084 |
| 9 | $-4.94^{+0.46}_{-0.31}$ | $-21.36^{+0.54}_{-0.38}$ | -2.35 | $25.12^{+0.16}_{-0.11}$ | – |
| 10 | $-5.79^{+1.1}_{-0.84}$ | $-21.8^{+1.6}_{-1.2}$ | -2.35 | $24.51^{+0.19}_{-0.15}$ | – |
| 12 | $-6.19^{+0.67}_{-1.3}$ | < -19.1 | -2.35 | $24.40^{+0.23}_{-0.12}$ | – |

Table 1. Constraints on luminosity density obtained from Schechter fit and the GP fit to the data at different redshifts between $2 < z < 8$. For $z = 9, 10, 12$ we just provide only the Schechter fit as even the three parameters can not be constrained with two tailed distribution from the data, due to low signal-to-noise ratio.

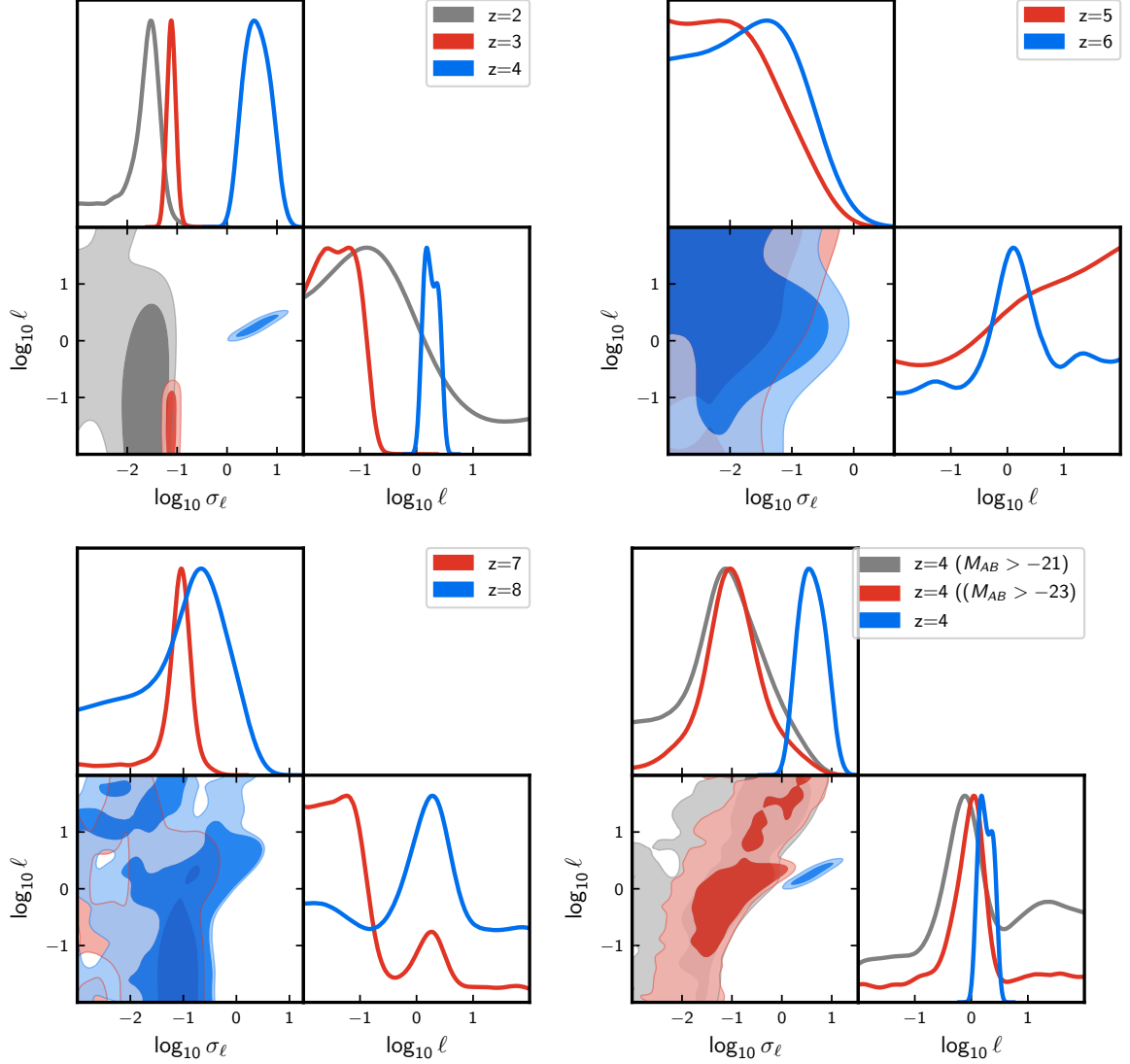


Figure 4. Constraints on the GP hyperparameters at different redshifts. Redshifts between $z = 2-12$ are divided into 3 plots. At lower redshifts, mainly at $z = 3$ and 4 , the data prefers significant deviation from the Schechter function. At higher redshifts, although there are some hints of deviations at $z = 7, 8$, they are not statistically significant. For $z = 4$, where we find most significant deviation, we reanalyze the data with two cuts $M_{UV} > -23$ and $M_{UV} > -21$ (bottom right plot). We notice that when we include the data from lower magnitudes, the Schechter function becomes increasingly inconsistent with the data.

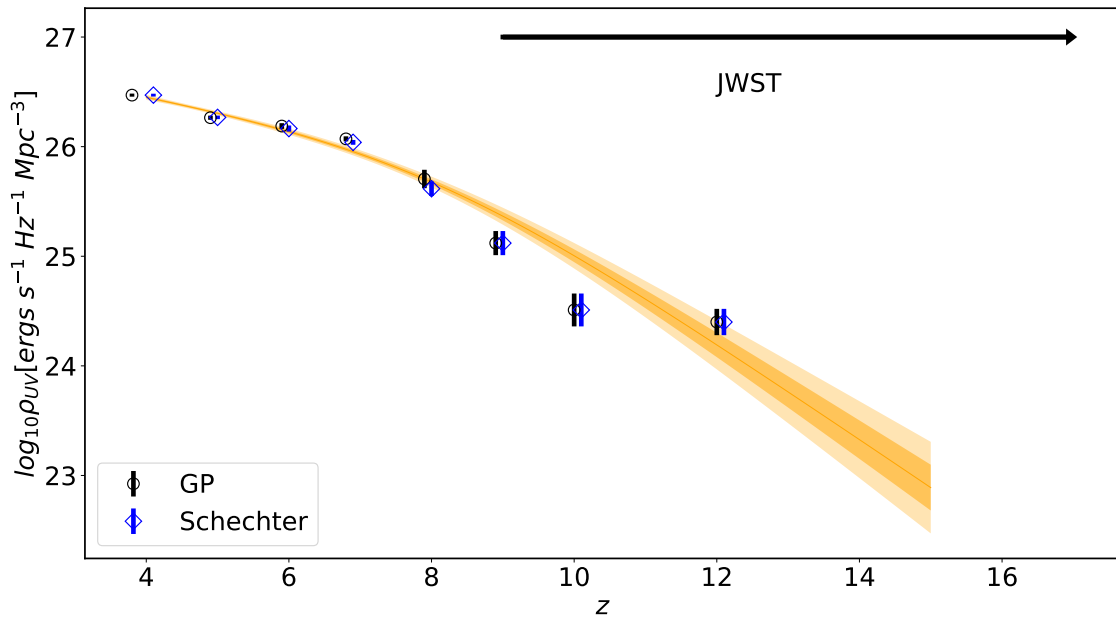


Figure 5. Luminosity density evolution across redshift $z \sim 4 - 12$. Black circles and blue diamonds are $\rho_{UV}(z)$ s obtained from integrating the luminosity functions from GP and Schechter respectively down to the magnitude $M_{UV} = -17$. The orange line is best-fit logarithmic double power-law. The shaded regions are 1σ and 2σ confidence level to the logarithmic double power-law fit to ρ_{UV} obtained from Schechter function fit.

the reionization process is mainly driven by fainter galaxies. The excess dropout galaxies at the brighter-end of magnitude have limited contribution to the reionization process due to lower number density or possibly low escape fraction. Earlier publications in [11, 50, 87–89] reached to a similar conclusions using model-based reionization study. As shown in Figure 6 we find much tighter bound of Q_{HII} as compared to previous works in [53, 56, 58, 87, 88]. We quote the midpoint (50%) redshift of reionization z_{re} in Table 2 which is less than the Planck reported value [4]. Our constraints on the duration of reionization (redshift difference between 10% to 90% reionization) are $\Delta z \sim 1.627^{+0.059}_{-0.071}$ and $1.627^{+0.060}_{-0.070}$ with 68% confidence interval using Schechter function and GP based ρ_{UV} data sets respectively. This is consistent with a upper bound of $\Delta z < 2.8$ as reported in [90] from the Kinetic Sunyaev–Zel’dovich effect. This implies our values suggest a sharper reionization history. Finally our constrain on reionization optical depth is $\tau_{\text{re}} = 0.0492^{+0.0008}_{-0.0006}$ and $0.0494^{+0.0007}_{-0.0006}$ from Schechter and GP analyses. These values are also listed in Table 2. However, we would like to highlight here that the uncertainties in the reionization histories quoted in this subsection are underestimated as we have fixed both the clumping factor and the escape fraction in our analyses. Therefore, these summary statistics on optical depth and the duration of reionization should be used with caution in any subsequent analysis. The exercise in this subsection has been performed to indicate that the constraints on the cosmology remain unaltered even though Schechter function is ruled out by the observational data. The flattening/increase in the luminosity density data at high redshifts as indicated by the JWST data in this analysis does not show an impact in the optical depth constraints as – (1) we have not used the very high redshift

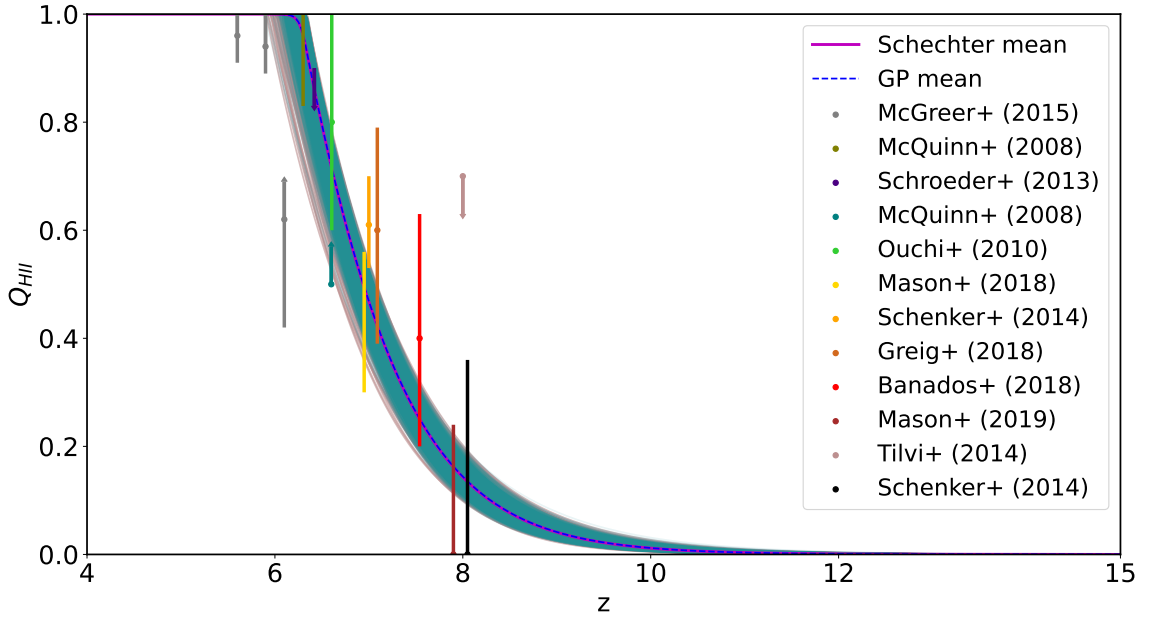


Figure 6. Redshift evolution of Q_{HII} across $z \sim 4 - 15$. The dashed blue and solid magenta lines are best-fit Q_{HII} estimated using ρ_{UVS} from GP and Schechter functions respectively. The gray (cyan) curves are random samples of Q_{HII} for these two respective cases. The Q_{HII} data sets used for joint fitting are also shown.

| | using $\log_{10}[\rho_{\text{UV}}]$ from Schechter | using $\log_{10}[\rho_{\text{UV}}]$ from GP |
|--------------------|--|---|
| τ_{re} | $0.0492^{+0.0008}_{-0.0006}$ | $0.0494^{+0.0007}_{-0.0006}$ |
| z_{re} | $6.778^{+0.054}_{-0.029}$ | $6.777^{+0.055}_{-0.028}$ |
| Δz | $1.627^{+0.059}_{-0.071}$ | $1.627^{+0.060}_{-0.070}$ |

Table 2. Summary of constraints on reionization history using ρ_{UV} data sets obtained from both parametric and non-parametric methods.

observations ($z \sim 14, 16$) from JWST, and (2) the double power-law form used for the luminosity density does not capture its increasing trend at high redshifts.

5 Summary

In this paper, we investigate the UV luminosity functions between redshifts $z \sim 2 - 12$ over a wide range of magnitude $-25 \lesssim M_{\text{UV}} \lesssim -14$ based on HST, HSC and JWST data sets. We test whether the conventional Schechter function is a valid theoretical model that can address the trends of luminosity data for such a wide range of magnitude and redshifts; and what are the implications of any modified function to the reionization history.

We fit both commonly used Schechter function model at all redshifts $z \sim 2 - 12$ and perform a free-form reconstruction at redshifts $z \sim 2 - 8$ using Gaussian process to the same

data sets. We find although Schechter function is a very good description of the dropout galaxies for the fainter end of magnitude ($M_{UV} \gtrsim -21$), its exponential tail is inconsistent with brighter dropout galaxies at almost all redshifts where low magnitude data are available. The Gaussian process regression allows a free-form reconstruction of UV LFs and therefore can well describe the excess LF at the bright-end which is not addressed by Schechter function. The GP hyperparameters confirms the rejection of Schechter function at high significance at redshifts $z = 3$ and 4. Analysis with the data below magnitude of -23 shows the significance is more than 3σ for $z = 4$. The luminosity data at $z = 2$ and 7 also disfavors the Schechter function at $\sim 95\%$ C.L. A hints of deviation from Schechter function for other redshifts is addressed with less significance due to unavailability of high quality data at low magnitudes. While these results are consistent with the deviation addressed in model dependent approaches of [26, 27, 29, 34] the GP LFs have also addressed the significant transient deviations from Schechter function $z = 3$ and 4 (Figure 2). We obtain the UV luminosity densities integrating over both LF forms down to the magnitude $M_{UV} = -17$. Since at the fainter end of the magnitude, Schechter function is consistent with the data and the fainter end contributes dominantly to the luminosity density integral due to the maximum availability of Galaxies, we find similar luminosity densities in both the methods. Therefore, reionization history is found to be similar in both cases. This implies that brighter dropout galaxies have insignificant contributions in reionization process (supported by earlier publications as well). However, integrating to more fainter sources $M_{UV} > -15$ can indicate certain differences which we do not explore by considering $M_{UV} = -17$ as the conservative choice.

The data at redshifts 9, 10 and 12 do not have a high signal-to-noise ratio and therefore can not constrain all the Schechter function parameters. Therefore testing a modification to Schechter function is beyond the scope of this paper with the available data. More observational data from JWST NIRSpec will be required for further studies at higher redshifts. Furthermore, we have not incorporated redshift dependencies of clumping factor and escape fraction into our simplistic reionization model and also neglect the contributions from quasars as reionization sources which could potentially enhance the accuracy of our findings. It would be intriguing to incorporate all these modifications into our model and reassess the current analysis when new data from JWST and other sources with significant improvement in the signal-to-noise ratio are made available. We defer these extensions for future investigations.

6 Acknowledgement

All the computations in this paper are done using the HPC Nandadevi and Kamet (<https://hpc.imsc.res.in>) at the Institute of Mathematical Sciences, Chennai, India. The authors would like to thank Yuichi Harikane for providing the UV luminosity data sets used in this work. DKH would like to thank Daniela Paoletti for certain important discussions. DKH would like to acknowledge the support from the Indo-French Centre for the Promotion of Advanced Research – CEFIPRA grant no. 6704-4 and the support through the India-Italy “RELIC - Reconstructing Early and Late events In Cosmology” mobility program.

A Modification to the mean functions due to changes in the hyperparameters

In this section we describe how GP performs over its hyperparameter space. The GP likelihood in terms of data \mathbf{y} for zero mean function and a given kernel covariance matrix $C(X, X)$

can be written as,

$$\log p(\mathbf{y}|X) = -\frac{1}{2}\mathbf{y}^T(C + \sigma_n^2\mathbf{I})\mathbf{y} - \frac{1}{2}\log|C + \sigma_n^2\mathbf{I}| - \frac{n}{2}\log(2\pi) \quad (\text{A.1})$$

where σ_n is the noise standard deviation at data points and n is the number of data points.

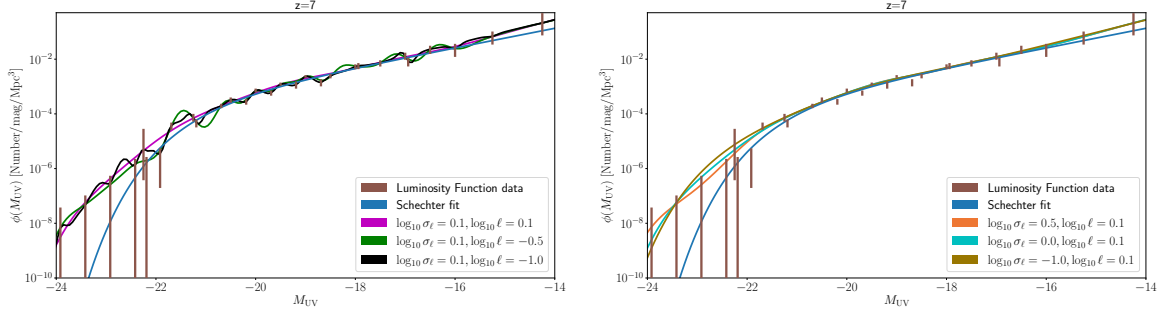


Figure 7. Schematic plot to show the effect of σ_ℓ and ℓ to construct LFs at redshift $z \sim 7$. The blue line shows Schechter best fit. Left panel: Highlights the role of correlation length ℓ . The black, green and magenta lines show the GP reconstructed LFs for three choice of $\log_{10} \ell = -1.0, -0.5$ and 0.1 respectively with fixed $\log_{10} \sigma_\ell = 0.1$. For low value of ℓ , LF is wiggly and with larger value of ℓ the LFs are smoother. Right panel: Highlights the role of σ_ℓ . The dark yellow, cyan and orange lines represent the LFs for $\log_{10} \sigma_\ell = -1, 0$ and 0.5 respectively for fixed $\log_{10} \ell = 0.1$. With different choice of σ_ℓ , a overall shift from initial mean function is seen.

The first term is similar to the χ^2 that tries to keep the GP functions as close as data points y by optimizing the kernel hyperparameters. The second term is the penalty term that is independent of data y and solely contributed by the kernel and this term tries to maximize the likelihood smoothing the small-scale features of GP functions by optimizing the correlation length hyperparameter ℓ . For optimized hyperparameters, GP generates the predictive mean functions at predictive points X_* for given mean function $\mu(X_*)$ following,

$$f(X_*) = \mu(X_*) + \mathbf{C}(X, X_*)\mathbf{C}_y^{-1}(\mathbf{y} - \mu(X)), \quad (\text{A.2})$$

where $\mathbf{C}_y = \mathbf{C}(X, X) + \sigma_n^2\mathbf{I}$.

Figure 7 illustrates the role of two GP hyperparameters ℓ and σ_ℓ . We choose the data set at redshift $z \sim 7$ as an example. In left panel, we present the role of correlation length hyperparameter ℓ . We display the LFs from GP for given best fit Schechter mean function (blue) for fixed $\log_{10} \sigma_\ell = 0.1$ and three different $\log_{10} \ell = 0.1$ (magenta), -0.5 (green) and -1.0 (black). For low value of $\log_{10} \ell = -1.0$, the reconstructed LF is wiggly. This choice of low correlation length is equivalent to imposing the condition to GP to prevent fitting the noise in data. With increase of correlation lengths for same σ_ℓ , the LFs become smoother. In right panel, we present the LFs for $\log_{10} \sigma_\ell = -1$ (dark yellow), 0.0 (cyan) and 0.1 (orange) for fixed $\log_{10} \ell = 0.1$. The curve shows an overall amplitude shift due to different choice of σ_ℓ which is evident below magnitude ~ -21 where best fit Schechter function starts sharp decay.

References

- [1] X. Fan, M.A. Strauss, R.H. Becker, R.L. White, J.E. Gunn, G.R. Knapp et al., *Constraining the Evolution of the Ionizing Background and the Epoch of Reionization with $z \sim 6$ Quasars. II. A Sample of 19 Quasars*, *AJ* **132** (2006) 117 [[astro-ph/0512082](#)].
- [2] I.D. McGreer, A. Mesinger and V. D’Odorico, *Model-independent evidence in favour of an end to reionization by $z \approx 6$* , *MNRAS* **447** (2015) 499 [[1411.5375](#)].
- [3] D.K. Hazra and G.F. Smoot, *Witnessing the reionization history using cosmic microwave background observation from planck*, *Journal of Cosmology and Astroparticle Physics* **2017** (2017) 028.
- [4] Planck Collaboration, N. Aghanim, Y. Akrami, M. Ashdown, J. Aumont, C. Baccigalupi et al., *Planck 2018 results. VI. Cosmological parameters*, *A&A* **641** (2020) A6 [[1807.06209](#)].
- [5] D. Paoletti, D.K. Hazra, F. Finelli and G.F. Smoot, *The asymmetry of dawn: evidence for asymmetric reionization histories from a joint analysis of cosmic microwave background and astrophysical data*, [2405.09506](#).
- [6] G. Worseck, J.X. Prochaska, J.F. Hennawi and M. McQuinn, *Early and Extended Helium Reionization over More Than 600 Million Years of Cosmic Time*, *ApJ* **825** (2016) 144 [[1405.7405](#)].
- [7] A. Fontana, E. Vanzella, L. Pentericci, M. Castellano, M. Giavalisco, A. Grazian et al., *The Lack of Intense Ly α in Ultradeep Spectra of $z = 7$ Candidates in GOODS-S: Imprint of Reionization?*, *ApJ* **725** (2010) L205 [[1010.2754](#)].
- [8] C.J. Willott, P. Delorme, C. Reyl  , L. Albert, J. Bergeron, D. Crampton et al., *The Canada-France High- z Quasar Survey: Nine New Quasars and the Luminosity Function at Redshift 6*, *AJ* **139** (2010) 906 [[0912.0281](#)].
- [9] M. Onoue, N. Kashikawa, C.J. Willott, P. Hibon, M. Im, H. Furusawa et al., *Minor Contribution of Quasars to Ionizing Photon Budget at $z \sim 6$: Update on Quasar Luminosity Function at the Faint End with Subaru/Suprime-Cam*, *ApJ* **847** (2017) L15 [[1709.04413](#)].
- [10] S. Hassan, R. Dav  , S. Mitra, K. Finlator, B. Ciardi and M.G. Santos, *Constraining the contribution of active galactic nuclei to reionization*, *Monthly Notices of the Royal Astronomical Society* **473** (2017) 227 [<https://academic.oup.com/mnras/article-pdf/473/1/227/21308514/stx2194.pdf>].
- [11] P. Dayal, M. Volonteri, T.R. Choudhury, R. Schneider, M. Trebitsch, N.Y. Gnedin et al., *Reionization with galaxies and active galactic nuclei*, *MNRAS* **495** (2020) 3065 [[2001.06021](#)].
- [12] C. Liu, S.J. Mutch, P.W. Angel, A.R. Duffy, P.M. Geil, G.B. Poole et al., *Dark-ages reionization and galaxy formation simulation – IV. UV luminosity functions of high-redshift galaxies*, *Monthly Notices of the Royal Astronomical Society* **462** (2016) 235 [<https://academic.oup.com/mnras/article-pdf/462/1/235/18468542/stw1015.pdf>].
- [13] T.R. Choudhury and A. Ferrara, *Experimental constraints on self-consistent reionization models*, *Monthly Notices of the Royal Astronomical Society* **361** (2005) 577 [<https://academic.oup.com/mnras/article-pdf/361/2/577/18660784/361-2-577.pdf>].
- [14] B.E. Robertson, *Estimating Luminosity Function Constraints from High-Redshift Galaxy Surveys*, *ApJ* **713** (2010) 1266 [[1001.1008](#)].
- [15] J.M. Lotz, A. Koekemoer, D. Coe, N. Grogin, P. Capak, J. Mack et al., *The Frontier Fields: Survey Design and Initial Results*, *ApJ* **837** (2017) 97 [[1605.06567](#)].
- [16] M.A. Schenker, B.E. Robertson, R.S. Ellis, Y. Ono, R.J. McLure, J.S. Dunlop et al., *The uv luminosity function of star-forming galaxies via dropout selection at redshifts $z \sim 7$ and 8 from the 2012 ultra deep field campaign*, *The Astrophysical Journal* **768** (2013) 196.

- [17] R.S. Ellis, R.J. McLure, J.S. Dunlop, B.E. Robertson, Y. Ono, M.A. Schenker et al., *The Abundance of Star-forming Galaxies in the Redshift Range 8.5-12: New Results from the 2012 Hubble Ultra Deep Field Campaign*, *ApJ* **763** (2013) L7 [1211.6804].
- [18] R.J. McLure, J.S. Dunlop, R.A.A. Bowler, E. Curtis-Lake, M. Schenker, R.S. Ellis et al., *A new multifield determination of the galaxy luminosity function at $z = 7-9$ incorporating the 2012 Hubble Ultra-Deep Field imaging*, *Monthly Notices of the Royal Astronomical Society* **432** (2013) 2696 [https://academic.oup.com/mnras/article-pdf/432/4/2696/9501883/stt627.pdf].
- [19] M. Ishigaki, R. Kawamata, M. Ouchi, M. Oguri, K. Shimasaku and Y. Ono, *Hubble Frontier Fields First Complete Cluster Data: Faint Galaxies at $z \sim 5-10$ for UV Luminosity Functions and Cosmic Reionization*, *Astrophys. J.* **799** (2015) 12 [1408.6903].
- [20] M. Ishigaki, R. Kawamata, M. Ouchi, M. Oguri, K. Shimasaku and Y. Ono, *Full-data Results of Hubble Frontier Fields: UV Luminosity Functions at $z \sim 6-10$ and a Consistent Picture of Cosmic Reionization*, *ApJ* **854** (2018) 73 [1702.04867].
- [21] R.J. Bouwens et al., *UV Luminosity Functions at redshifts $z \sim 4$ to $z \sim 10$: 10000 Galaxies from HST Legacy Fields*, *Astrophys. J.* **803** (2015) 34 [1403.4295].
- [22] P. Schechter, *An analytic expression for the luminosity function for galaxies.*, *ApJ* **203** (1976) 297.
- [23] J. Loveday, P. Norberg, I.K. Baldry, S.P. Driver, A.M. Hopkins, J.A. Peacock et al., *Galaxy and Mass Assembly (GAMA): ugriz galaxy luminosity functions*, *Monthly Notices of the Royal Astronomical Society* **420** (2012) 1239 [https://academic.oup.com/mnras/article-pdf/420/2/1239/3065107/mnras0420-1239.pdf].
- [24] R.G. Bower, A.J. Benson, R. Malbon, J.C. Helly, C.S. Frenk, C.M. Baugh et al., *Breaking the hierarchy of galaxy formation*, *Monthly Notices of the Royal Astronomical Society* **370** (2006) 645 [https://academic.oup.com/mnras/article-pdf/370/2/645/2898993/mnras0370-0645.pdf].
- [25] A.J. Benson, R.G. Bower, C.S. Frenk, C.G. Lacey, C.M. Baugh and S. Cole, *What Shapes the Luminosity Function of Galaxies?*, *ApJ* **599** (2003) 38 [astro-ph/0302450].
- [26] Y. Ono, M. Ouchi, Y. Harikane, J. Toshikawa, M. Rauch, S. Yuma et al., *Great Optically Luminous Dropout Research Using Subaru HSC (GOLDRUSH). I. UV luminosity functions at $z \sim 4-7$ derived with the half-million dropouts on the 100 deg² sky*, *PASJ* **70** (2018) S10 [1704.06004].
- [27] M.L. Stevans, S.L. Finkelstein, I. Wold, L. Kawinwanichakij, C. Papovich, S. Sherman et al., *Bridging Star-forming Galaxy and AGN Ultraviolet Luminosity Functions at $z = 4$ with the SHELA Wide-field Survey*, *ApJ* **863** (2018) 63 [1806.05187].
- [28] N.J. Adams, R.A.A. Bowler, M.J. Jarvis, B. Häußler, R.J. McLure, A. Bunker et al., *The rest-frame UV luminosity function at $z \simeq 4$: a significant contribution of AGNs to the bright end of the galaxy population*, *MNRAS* **494** (2020) 1771 [1912.01626].
- [29] Y. Harikane, A.K. Inoue, K. Mawatari, T. Hashimoto, S. Yamanaka, Y. Fudamoto et al., *A search for h-dropout lyman break galaxies at $z \sim 12-16$* , *The Astrophysical Journal* **929** (2022) 1.
- [30] R.A.A. Bowler, J.S. Dunlop, R.J. McLure, H.J. McCracken, B. Milvang-Jensen, H. Furusawa et al., *Discovery of bright $z \simeq 7$ galaxies in the UltraVISTA survey*, *Monthly Notices of the Royal Astronomical Society* **426** (2012) 2772 [https://academic.oup.com/mnras/article-pdf/426/4/2772/3299565/426-4-2772.pdf].
- [31] J.S.B. Wyithe, H. Yan, R.A. Windhorst and S. Mao, *A distortion of very-high-redshift galaxy number counts by gravitational lensing*, *Nature* **469** (2011) 181 [1101.2291].

- [32] J. Rigby, M. Perrin, M. McElwain, R. Kimble, S. Friedman, M. Lallo et al., *The Science Performance of JWST as Characterized in Commissioning*, *PASP* **135** (2023) 048001 [2207.05632].
- [33] M. Stefanon, I. Labbé, R.J. Bouwens, P. Oesch, M.L.N. Ashby, K.I. Caputi et al., *The Brightest $z \gtrsim 8$ Galaxies over the COSMOS UltraVISTA Field*, *ApJ* **883** (2019) 99 [1902.10713].
- [34] R.A.A. Bowler, M.J. Jarvis, J.S. Dunlop, R.J. McLure, D.J. McLeod, N.J. Adams et al., *A lack of evolution in the very bright end of the galaxy luminosity function from $z \simeq 8$ to 10*, *MNRAS* **493** (2020) 2059 [1911.12832].
- [35] R. Takahashi, M. Oguri, M. Sato and T. Hamana, *Probability distribution functions of cosmological lensing: Convergence, shear, and magnification*, *The Astrophysical Journal* **742** (2011) 15.
- [36] R.L. Barone-Nugent, J.S.B. Wyithe, M. Trenti, T. Treu, P. Oesch, R. Bouwens et al., *The impact of strong gravitational lensing on observed Lyman-break galaxy numbers at $4 \leq z \leq 8$ in the GOODS and the XDF blank fields*, *MNRAS* **450** (2015) 1224 [1502.03887].
- [37] R. Barkana and A. Loeb, *In the beginning: the first sources of light and the reionization of the universe*, *Phys. Rep.* **349** (2001) 125 [astro-ph/0010468].
- [38] M. Kuhlen and C.-A. Faucher-Giguère, *Concordance models of reionization: implications for faint galaxies and escape fraction evolution*, *Monthly Notices of the Royal Astronomical Society* **423** (2012) 862 [https://academic.oup.com/mnras/article-pdf/423/1/862/18612580/mnras0423-0862.pdf].
- [39] B.E. Robertson, S.R. Furlanetto, E. Schneider, S. Charlot, R.S. Ellis, D.P. Stark et al., *New Constraints on Cosmic Reionization from the 2012 Hubble Ultra Deep Field Campaign*, *ApJ* **768** (2013) 71 [1301.1228].
- [40] I.T. Iliev, G. Mellema, U.L. Pen, H. Merz, P.R. Shapiro and M.A. Alvarez, *Simulating cosmic reionization at large scales - I. The geometry of reionization*, *MNRAS* **369** (2006) 1625 [astro-ph/0512187].
- [41] A.H. Pawlik, J. Schaye and E. van Scherpenzeel, *Keeping the Universe ionized: photoheating and the clumping factor of the high-redshift intergalactic medium*, *MNRAS* **394** (2009) 1812 [0807.3963].
- [42] K. Finlator, S.P. Oh, F. Özel and R. Davé, *Gas clumping in self-consistent reionization models*, *Monthly Notices of the Royal Astronomical Society* **427** (2012) 2464 [https://academic.oup.com/mnras/article-pdf/427/3/2464/3857876/427-3-2464.pdf].
- [43] J. Schroeder, A. Mesinger and Z. Haiman, *Evidence of Gunn-Peterson damping wings in high- z quasar spectra: strengthening the case for incomplete reionization at $z \sim 6-7$* , *MNRAS* **428** (2013) 3058 [1204.2838].
- [44] J.M. Shull, A. Harness, M. Trenti and B.D. Smith, *Critical star formation rates for reionization: Full reionization occurs at redshift $z=7$* , *The Astrophysical Journal* **747** (2012) 100.
- [45] B.E. Robertson, *Galaxy formation and reionization: Key unknowns and expected breakthroughs by the James Webb Space Telescope*, *Annual Review of Astronomy and Astrophysics* **60** (2022) 121 [https://doi.org/10.1146/annurev-astro-120221-044656].
- [46] A.K. Inoue, I. Shimizu, I. Iwata and M. Tanaka, *An updated analytic model for attenuation by the intergalactic medium*, *MNRAS* **442** (2014) 1805 [1402.0677].
- [47] E.R. Fernandez and J.M. Shull, *The effect of galactic properties on the escape fraction of ionizing photons*, *The Astrophysical Journal* **731** (2011) 20.

- [48] C.A. Mason, T. Treu, M. Dijkstra, A. Mesinger, M. Trenti, L. Pentericci et al., *The Universe Is Reionizing at $z \sim 7$: Bayesian Inference of the IGM Neutral Fraction Using Ly α Emission from Galaxies*, *Astrophys. J.* **856** (2018) 2 [1709.05356].
- [49] X. Ma, D. Kasen, P.F. Hopkins, C.-A. Faucher-Gigu re, E. Quataert, D. Kere si et al., *The difficulty of getting high escape fractions of ionizing photons from high-redshift galaxies: a view from the FIRE cosmological simulations*, *Monthly Notices of the Royal Astronomical Society* **453** (2015) 960 [<https://academic.oup.com/mnras/article-pdf/453/1/960/4935561/stv1679.pdf>].
- [50] H. Atek, I. Labb e, L.J. Furtak, I. Chemerynska, S. Fujimoto, D.J. Setton et al., *Most of the photons that reionized the Universe came from dwarf galaxies*, *Nature* **626** (2024) 975 [2308.08540].
- [51] C. Simmonds, S. Tacchella, K. Hainline, B.D. Johnson, W. McClymont, B. Robertson et al., *Low-mass bursty galaxies in JADES efficiently produce ionizing photons and could represent the main drivers of reionization*, *MNRAS* **527** (2024) 6139 [2310.01112].
- [52] J.B. Mu noz, J. Mirocha, J. Chisholm, S.R. Furlanetto and C. Mason, *Reionization after JWST: a photon budget crisis?*, *arXiv e-prints* (2024) arXiv:2404.07250 [2404.07250].
- [53] S. Mitra and A. Chatterjee, *Non-parametric reconstruction of photon escape fraction from reionization*, *MNRAS* **523** (2023) L35 [2303.02704].
- [54] C.-A. Faucher-Gigu re, D. Kere si and C.-P. Ma, *The baryonic assembly of dark matter haloes*, *Monthly Notices of the Royal Astronomical Society* **417** (2011) 2982 [<https://academic.oup.com/mnras/article-pdf/417/4/2982/3842290/mnras0417-2982.pdf>].
- [55] Y.-W. Yu, K. Cheng, M. Chu and S. Yeung, *Cosmic histories of star formation and reionization: an analysis with a power-law approximation*, *Journal of Cosmology and Astroparticle Physics* **2012** (2012) 023.
- [56] D.K. Hazra, D. Paoletti, F. Finelli and G.F. Smoot, *Joining bits and pieces of reionization history*, *Phys. Rev. Lett.* **125** (2020) 071301.
- [57] D. Paoletti, D.K. Hazra, F. Finelli and G.F. Smoot, *Extended reionization in models beyond Λ CDM with Planck 2018 data*, *JCAP* **09** (2020) 005 [2005.12222].
- [58] A. Krishak and D.K. Hazra, *Gaussian process reconstruction of reionization history*, *The Astrophysical Journal* **922** (2021) 95.
- [59] D. Paoletti, D.K. Hazra, F. Finelli and G.F. Smoot, *Dark twilight joined with the light of dawn to unveil the reionization history*, *Phys. Rev. D* **104** (2021) 123549 [2107.10693].
- [60] M. Seikel, C. Clarkson and M. Smith, *Reconstruction of dark energy and expansion dynamics using gaussian processes*, *Journal of Cosmology and Astroparticle Physics* **2012** (2012) 036.
- [61] A. Shafieloo, A.G. Kim and E.V. Linder, *Model independent tests of cosmic growth versus expansion*, *Phys. Rev. D* **87** (2013) 023520.
- [62] R. Calderon, A. Shafieloo, D. Kumar Hazra and W. Sohn, *On the consistency of Λ CDM with CMB measurements in light of the latest Planck, ACT and SPT data*, *J. Cosmology Astropart. Phys.* **2023** (2023) 059 [2302.14300].
- [63] C.E. Rasmussen and C.K.I. Williams, *Gaussian processes for machine learning.*, Adaptive computation and machine learning, MIT Press (2006).
- [64] R.J. Bouwens, P.A. Oesch, M. Stefanon, G. Illingworth, I. Labb e, N. Reddy et al., *New Determinations of the UV Luminosity Functions from $z = 9$ to $z = 2$ Show a Remarkable Consistency with Halo Growth and a Constant Star Formation Efficiency*, *AJ* **162** (2021) 47 [2102.07775].
- [65] Y. Harikane, Y. Ono, M. Ouchi, C. Liu, M. Sawicki, T. Shibuya et al., *GOLDRUSH. IV. Luminosity Functions and Clustering Revealed with 4,000,000 Galaxies at $z = 2-7$: Galaxy-AGN*

- Transition, Star Formation Efficiency, and Implication for Evolution at $z \gtrsim 10$* , *ApJS* **259** (2022) 20 [2108.01090].
- [66] P.A. Oesch, R.J. Bouwens, G.D. Illingworth, I. Labbé and M. Stefanon, *The dearth of $z \sim 10$ galaxies in all hst legacy fields—the rapid evolution of the galaxy population in the first 500 myr*, *The Astrophysical Journal* **855** (2018) 105.
- [67] D.J. McLeod, R.J. McLure and J.S. Dunlop, *The $z = 9-10$ galaxy population in the Hubble Frontier Fields and CLASH surveys: the $z = 9$ luminosity function and further evidence for a smooth decline in ultraviolet luminosity density at $z \geq 8$* , *MNRAS* **459** (2016) 3812 [1602.05199].
- [68] Y. Harikane, M. Ouchi, M. Oguri, Y. Ono, K. Nakajima, Y. Isobe et al., *A Comprehensive Study of Galaxies at z 9-16 Found in the Early JWST Data: Ultraviolet Luminosity Functions and Cosmic Star Formation History at the Pre-reionization Epoch*, *ApJS* **265** (2023) 5 [2208.01612].
- [69] Y. Ono et al., *Spectroscopic Confirmation of Three z -Dropout Galaxies at $z = 6.844 - 7.213$: Demographics of Lyman-Alpha Emission in $z \sim 7$ Galaxies*, *Astrophys. J.* **744** (2012) 83 [1107.3159].
- [70] V. Tilvi, C. Papovich, S.L. Finkelstein, J. Long, M. Song, M. Dickinson et al., *Rapid Decline of Ly α Emission Toward the Reionization Era*, *Astrophys. J.* **794** (2014) 5 [1405.4869].
- [71] M.A. Schenker, R.S. Ellis, N.P. Konidaris and D.P. Stark, *Line Emitting Galaxies Beyond a Redshift of 7: An Improved Method for Estimating the Evolving Neutrality of the Intergalactic Medium*, *Astrophys. J.* **795** (2014) 20 [1404.4632].
- [72] B. Greig, A. Mesinger, Z. Haiman and R.A. Simcoe, *Are we witnessing the epoch of reionization at $z=7.1$ from the spectrum of J1120+0641?*, *Mon. Not. Roy. Astron. Soc.* **466** (2017) 4239 [1606.00441].
- [73] F.B. Davies et al., *Quantitative Constraints on the Reionization History from the IGM Damping Wing Signature in Two Quasars at $z \gtrsim 7$* , *Astrophys. J.* **864** (2018) 142 [1802.06066].
- [74] T. Totani, N. Kawai, G. Kosugi, K. Aoki, T. Yamada, M. Iye et al., *Implications for the cosmic reionization from the optical afterglow spectrum of the gamma-ray burst 050904 at $z = 6.3$* , *Publ. Astron. Soc. Jap.* **58** (2006) 485 [astro-ph/0512154].
- [75] M. McQuinn, A. Lidz, M. Zaldarriaga, L. Hernquist and S. Dutta, *Probing the neutral fraction of the IGM with GRBs during the epoch of reionization*, *MNRAS* **388** (2008) 1101 [0710.1018].
- [76] J.S. Bolton, M.G. Haehnelt, S.J. Warren, P.C. Hewett, D.J. Mortlock, B.P. Venemans et al., *How neutral is the intergalactic medium surrounding the redshift $z = 7.085$ quasar ULAS J1120+0641?*, *MNRAS* **416** (2011) L70 [1106.6089].
- [77] D.J. Mortlock, S.J. Warren, B.P. Venemans, M. Patel, P.C. Hewett, R.G. McMahon et al., *A luminous quasar at a redshift of $z = 7.085$* , *Nature* **474** (2011) 616 [1106.6088].
- [78] A. Lewis and S. Bridle, *Cosmological parameters from CMB and other data: A Monte Carlo approach*, *Phys. Rev.* **D66** (2002) 103511 [astro-ph/0205436].
- [79] S.L. Finkelstein, R.E. Ryan, C. Papovich, M. Dickinson, M. Song, R.S. Somerville et al., *The evolution of the galaxy rest-frame ultraviolet luminosity function over the first two billion years*, *The Astrophysical Journal* **810** (2015) 71.
- [80] E. Glikman, S.G. Djorgovski, D. Stern, A. Dey, B.T. Jannuzi and K.-S. Lee, *The faint end of the quasar luminosity function at $z \sim 4$: Implications for ionization of the intergalactic medium and cosmic downsizing**, *The Astrophysical Journal Letters* **728** (2011) L26.
- [81] E. Giallongo, A. Grazian, F. Fiore, A. Fontana, L. Pentericci, E. Vanzella et al., *Faint AGNs at $z \gtrsim 4$ in the CANDELS GOODS-S field: looking for contributors to the reionization of the Universe*, *A&A* **578** (2015) A83 [1502.02562].

- [82] M. Niida, T. Nagao, H. Ikeda, K. Matsuoka, M.A.R. Kobayashi, Y. Toba et al., *Revisiting the completeness and luminosity function in high-redshift low-luminosity quasar surveys*, *The Astrophysical Journal* **832** (2016) 208.
- [83] M. Akiyama, W. He, H. Ikeda, M. Niida, T. Nagao, J. Bosch et al., *The quasar luminosity function at redshift 4 with the Hyper Suprime-Cam Wide Survey*, *Publications of the Astronomical Society of Japan* **70** (2017) [<https://academic.oup.com/pasj/article-pdf/70/SP1/S34/23692427/psx091.pdf>].
- [84] S. Parsa, J.S. Dunlop and R.J. McLure, *No evidence for a significant AGN contribution to cosmic hydrogen reionization*, *Monthly Notices of the Royal Astronomical Society* **474** (2017) 2904 [<https://academic.oup.com/mnras/article-pdf/474/3/2904/22843311/stx2887.pdf>].
- [85] S.L. Finkelstein, M.B. Bagley, H.C. Ferguson, S.M. Wilkins, J.S. Kartaltepe, C. Papovich et al., *CEERS Key Paper. I. An Early Look into the First 500 Myr of Galaxy Formation with JWST*, *ApJ* **946** (2023) L13 [[2211.05792](https://arxiv.org/abs/2211.05792)].
- [86] D.J. Eisenstein, C. Willott, S. Alberts, S. Arribas, N. Bonaventura, A.J. Bunker et al., *Overview of the JWST Advanced Deep Extragalactic Survey (JADES)*, *arXiv e-prints* (2023) [[arXiv:2306.02465](https://arxiv.org/abs/2306.02465)] [[2306.02465](https://arxiv.org/abs/2306.02465)].
- [87] S. Mitra, T.R. Choudhury and A. Ferrara, *Cosmic reionization after Planck.*, *MNRAS* **454** (2015) L76 [[1505.05507](https://arxiv.org/abs/1505.05507)].
- [88] S. Mitra, T.R. Choudhury and B. Ratra, *First study of reionization in the Planck 2015 normalized closed Λ CDM inflation model*, *MNRAS* **479** (2018) 4566 [[1712.00018](https://arxiv.org/abs/1712.00018)].
- [89] S.L. Finkelstein, A. D’Aloisio, J.-P. Paardekooper, J. Ryan, Russell, P. Behroozi, K. Finlator et al., *Conditions for Reionizing the Universe with a Low Galaxy Ionizing Photon Escape Fraction*, *ApJ* **879** (2019) 36 [[1902.02792](https://arxiv.org/abs/1902.02792)].
- [90] Planck Collaboration, R. Adam, N. Aghanim, M. Ashdown, J. Aumont, C. Baccigalupi et al., *Planck intermediate results. XLVII. Planck constraints on reionization history*, *A&A* **596** (2016) A108 [[1605.03507](https://arxiv.org/abs/1605.03507)].